

# Effects of the Solubility Parameter of Polyimides and the Segment Length of Siloxane Block on the Morphology and Properties of Poly(imide siloxane)

SHYI-LIANG JWO,<sup>1</sup> WHA-TZONG WHANG,<sup>1</sup> WEN-CHANG LIAW<sup>2</sup>

<sup>1</sup> Department of Materials Science and Engineering, National Chiao Tung University, Hsin Chu 300, Taiwan, Republic of China

<sup>2</sup> Department of Chemical Engineering, National Yunlin University of Science and Technology, 123, Section 3, Ta Hsueh Road, Tonliu, Yunlin 640, Taiwan, Republic of China

Received 24 December 1998; accepted 12 May 1999

**ABSTRACT:** The dependence of morphology of the poly(imide siloxane)s (PISs) on the solubility parameter of unmodified polyimides and the molecular weight and content of  $\alpha,\omega$ -bis(3-aminopropyl) polydimethylsiloxane (APPS) has been studied. The effect of the morphology on the mechanical properties is also under investigation. The domain formation in the PISs with the APPS molecular weight  $M_n = 507$  g/mol is not found until the mol ratio of APPS/PIS  $\geq 0.5\%$  in the pyromellitic dianhydride/*p*-phenylene diamine (PMDA/*p*-PDA)-based PISs, and at a mol ratio  $\geq 2.7\%$  in the 3,3',4,4'-benzophenone tetracarboxylic dianhydride/2,2'-bis[4-(3-aminophenoxy) phenyl] sulfone (BTDA/*m*-BAPS)-based PISs. As the APPS  $M_n = 715$  g/mol, the critical APPS concentrations of the domain formation in both types of PISs are equal to 0.1 and 1.1%, respectively. The critical concentration is equal to 0.6% in the BTDA/*m*-BAPS-based PIS film with the APPS  $M_n = 996$  g/mol. The isolated siloxane-rich phase in the BTDA/*m*-BAPS-based PISs becomes a continuous phase as the mol ratio of APPS/PIS  $\geq 7.7, 10.0,$  and  $16.6\%$  as the APPS  $M_n = 996, 715,$  and  $507$  g/mol, respectively. Dynamic Mechanical Analysis (DMA) shows two  $T_g$ s in the PIS films having phase separation: one at  $-118 \sim -115^\circ\text{C}$ , being the siloxane-rich phase, the other at  $181\text{--}244^\circ\text{C}$ , being the aromatic imide-rich phase. The SEM micrographs show a significant deformation on the fractured surfaces of the BTDA/*m*-BAPS-based PIS films with a continuous siloxane-rich phase. This phenomenon of plastic deformation is also observed in the tensile tests at  $-118^\circ\text{C}$  and at room temperature. The highest elongation in the PIS films is found at the critical siloxane content of the continuous siloxane-rich phase formation. © 1999 John Wiley & Sons, Inc. *J Appl Polym Sci* 74: 2832–2847, 1999

**Key words:** poly(imide siloxane)s; morphology; phase separation; plastic deformation

## INTRODUCTION

Polyimides, being thermally stable and mechanically tough, have been widely utilized in electronic and microelectronic industries<sup>1–4</sup> and aero-

space fields.<sup>5–7</sup> In addition to controlling glass transition temperature ( $T_g$ ) and processability, polyimides are usually modified with a siloxane segment to confer the excellent interfacial adhesion on the polyimide/substrate interface.<sup>4,8–11</sup> Siloxane-modified polyimides, called poly(imide siloxane)s, are block copolymers, consisting of imide and siloxane blocks. In 1966, Kuckertz<sup>12</sup> first reported poly(imide siloxane), which was prepared from PMDA with various low molecular weight amine-terminated siloxane dimers. Sum-

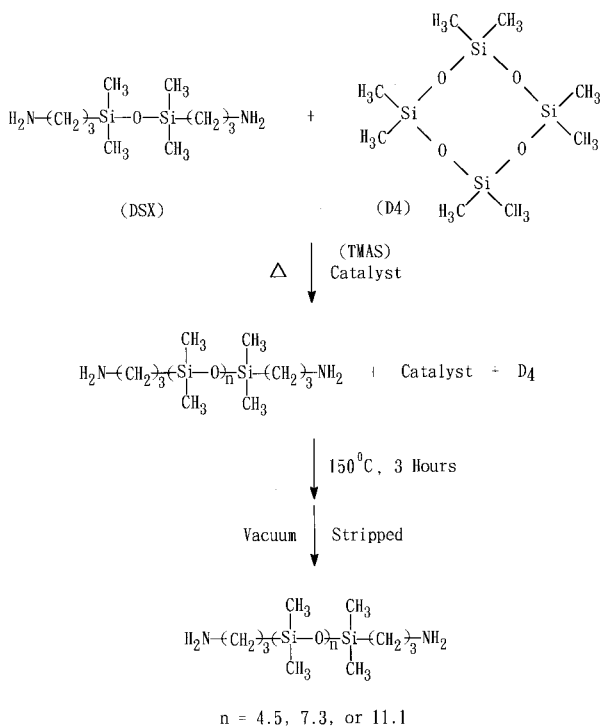
Correspondence to: W.-T. Whang.

Contract grant sponsors: National Science Council of the Republic of China, and the China Petroleum Company; contract grant number: NSC 87-CPC-1-009-008.

*Journal of Applied Polymer Science*, Vol. 74, 2832–2847 (1999)

© 1999 John Wiley & Sons, Inc.

CCC 0021-8995/99/122832-16

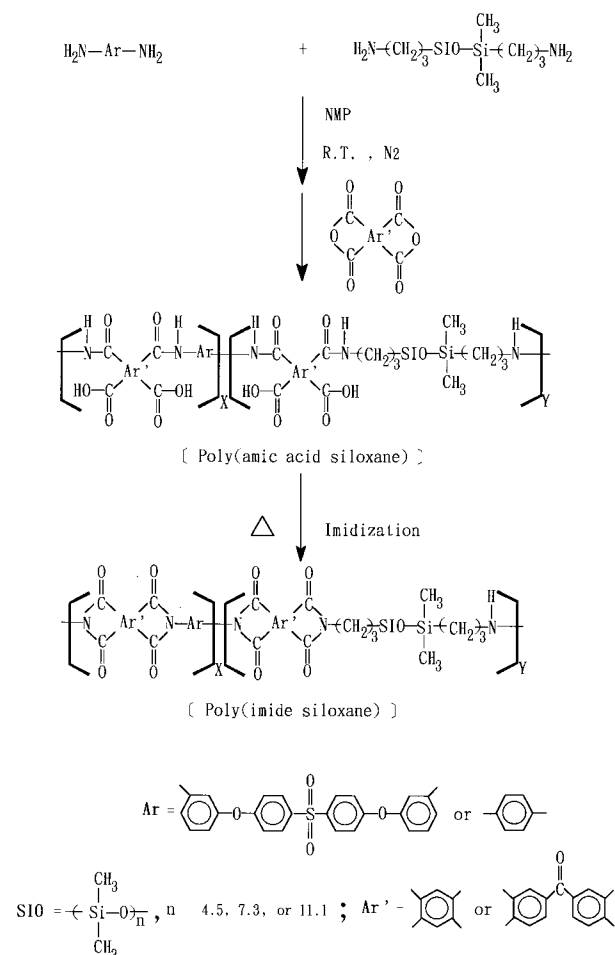


Scheme I

mers<sup>13</sup> synthesized poly(imide siloxane) by incorporating the APPS with various ratios (5, 10, 20, and 40 wt %) and different molecular weights ( $M_n = 900\text{--}10,000$  g/mol) into the BTDA and 3,3'-diaminodiphenyl sulfone (3,3'-DDS)-based polyimide. The modification of the siloxane segment did provide several desired improvements in the bulk and surface properties. Ube Industries, Ltd. developed a heat-resistant siloxane-modified polyimide from 3,3',4,4'-biphenyltetracarboxylic dianhydride (BPDA) and aromatic diamines and diaminopolysiloxane. The quantity and the segment length of the siloxane block affected the properties. Two  $T_g$ 's were found in the BPDA-based poly(imide siloxane) when the siloxane content was not less than 3 wt %. The APPS-modified polyimides of Sumitomo Bakelite Co., Ltd. (commercial name SIM) are used as a heat-resistant adhesive tape.<sup>4</sup> The dianhydrides for the SIM include 4,4'-oxydiphthalic anhydride (OPDA), PMDA, BTDA, BPDA, and the diamines include APPS and 1,3-bis(3-aminophenoxy)benzene.

Almost all of the studies for poly(imide siloxane) mainly focused on the relations between the content and the molecular weight of the siloxane segment and the mechanical, electrical, permeation,<sup>14</sup> thermal, and surface properties. The studies did not focus on the microphase or adequately explain the existence of microphase sep-

aration in the poly(imide siloxane) by thermal analysis and electron microscopy. It is known that the morphology or phase separation in a copolymer is affected by the compatibility of the segment. The physical or surface properties of the copolymer are related to their morphologies. However, systematic studies on the correlation of the morphologies of poly(imide siloxane) with the compatibility of segment components and the molecular weight and content of APPS is not available. In this study, the solubility parameters of the component segments of poly(imide siloxane)s are theoretically evaluated to understand the segment compatibility. After the evaluation, the first series of poly(imide siloxane)s are prepared from BTDA, *m*-BAPS, and APPS with various APPS contents and three APPS molecular weights. The second series of poly(imide siloxane)s are prepared as a reference from PMDA, *p*-PDA, and APPS. Their morphology is studied with a polarizing optical microscope (POM) and a scanning electron microscope (SEM). The mechanical prop-



Scheme II

**Table I** The Estimated Solubility Parameters ( $\delta$ )<sup>20</sup> and Glass Transition Temperatures ( $T_g$ ) of Various Polyimides from Diamines and Dianhydrides

Characteristics	BTDA		PMDA		BPDA		ODPA		6FDA <sup>a</sup>	
	$T_g$ , °C	$\delta$	$T_g$ , °C	$\delta$	$T_g$ , °C	$\delta$	$T_g$ , °C	$\delta$	$T_g$ , °C	$\delta$
Diamine <sup>b</sup>										
<i>m</i> -BAPS	252 <sup>c</sup> (224) <sup>21</sup>	30.6	286 <sup>c</sup> (254) <sup>21</sup>	31.2	235 <sup>21</sup>	30.2	244 <sup>c</sup> (211) <sup>21</sup>	30.3	236 <sup>21</sup>	27.1
	— <sup>d</sup>	19.7	—	18.5	—	19.2	—	19.3	—	18.3
<i>n</i> = 4.5	—	17.7	—	16.8	—	17.3	—	17.4	—	16.8
APPS <i>n</i> = 7.3	—	16.3	—	15.6	—	16.0	—	16.1	—	15.7
<i>n</i> = 11.1	—	16.3	—	15.6	—	16.0	—	16.1	—	15.7
<i>m</i> -BAPE	192 <sup>21</sup>	30.3	212 <sup>21</sup>	30.8	199 <sup>21</sup>	29.9	181 <sup>21</sup>	29.9	200 <sup>21</sup>	26.6
<i>m</i> -ODA	—	32.7	—	34.6	—	32.2	205 <sup>21</sup>	32.2	—	27.2
<i>m</i> -MDA	265 <sup>22</sup>	31.9	308 <sup>22</sup>	33.4	—	31.4	258 <sup>22</sup>	31.4	248 <sup>22</sup>	26.7
<i>m</i> -DABP	259 <sup>22</sup>	33.2	326 <sup>22</sup>	35.1	—	32.8	248 <sup>22</sup>	32.7	260 <sup>22</sup>	27.7
<i>m</i> -PDA	300 <sup>22</sup>	33.1	442 <sup>22</sup>	35.8	—	32.6	313 <sup>22</sup>	32.5	303 <sup>22</sup>	26.6
<i>p</i> -PDA	333 <sup>22</sup>	33.1	—	35.8	—	32.6	342 <sup>22</sup>	32.5	339 <sup>22</sup>	26.6
<i>m</i> -6F-diamine	239 <sup>23</sup>	27.7	—	27.7	267 <sup>23</sup>	27.1	224 <sup>23</sup>	27.2	250 <sup>23</sup>	24.1

<sup>a</sup> 6 FDA: 2,2'-bis-(3,4-dicarboxy phenyl) hexafluoropropane dianhydride.

<sup>b</sup> *m*-BAPE: 4,4'-bis(3-aminophenoxy) diphenyl ether; *m*-ODA: 3,3'-diaminodiphenyl ether; *m*-MDA: 3,3'-diaminodiphenylmethane; *m*-DABP: 3,3'-diaminobenzophenone; *m*-6F-diamine: 2,2'-bis(3-aminophenyl)hexafluoropropane; *m*-PDA: *m*-phenylene diamine; *p*-PDA: *p*-phenylene diamine.

<sup>c</sup> The data measured by DMA in our laboratory.

<sup>d</sup> Not determined.

erties are studied with a dynamic mechanical analyzer (DMA).

## EXPERIMENTAL

### Materials and Their Purification

High-purity octamethylcyclotetrasiloxane (D4, purity >97%), 1,3-bis(3-aminopropyl)-1,1,3,3-tetramethyldisiloxane (DSX, purity >97%) from United Chemical Technologies, and tetramethylammonium hydroxide pentahydrate (purity >98%) from Lancaster Synthesis Ltd. were used in the synthesis without further purification. BTDA (Aldrich Co.) and PMDA from Chris-Kev Co. were purified by recrystallization from a high-purity acetic anhydride, and then dried in a vacuum oven at 120°C for at least 14 h. The *m*-BAPS (Chriskev Co.) in high purity (99.23%) and *p*-PDA (purity >97%) from Tokyo Chemical Ind. Co. were heated in a vacuum oven at 90°C for 3 h prior to use. *N*-Methyl-2-pyrrolidone (NMP, Tedia Company) was dried over molecular sieves.

### Synthesis of APPS Oligomers

The catalyst tetramethylammonium siloxanolate (TMAS) was prepared from 4.31 g (0.0233 mol) of

tetramethylammonium hydroxide pentahydrate and 32.11 g (0.1050 mol) of D4 in a three-neck flask with magnetic stirring at 62–66°C under a strong argon stream for about 48 h.<sup>15–17</sup> The argon stream was bubbled through the reaction solution to remove the water completely. After the completion of the dehydration, a viscous translucent siloxanolate catalyst was obtained and stored in a refrigerator before the synthesis of APPS oligomer.

Three APPS oligomers were synthesized by an equilibration polymerization<sup>12,18,19</sup> involving DSX and D4 in the presence of the siloxanolate catalyst. The reactions are shown in Scheme I.

Three APPS oligomers were synthesized with the molecular weights equal to 507, 715, and 996 g/mol, respectively, corresponding to *n* = 4.5, 7.3, and 11.1, respectively. The APPS oligomer of molecular weight 507 g/mol was prepared from first heating the mixture of 8.42 g (0.0339 mol) of DSX along with 4.99 g (0.0168 mol) of D4 to 80°C in a flask with a nitrogen stream, and then adding 0.13 g (~ 1.0 wt %) of a tetramethylammonium siloxanolate catalyst into the mixture. The reaction was conducted at 80°C for 48 h, and then raised to 150°C for 3 h to decompose the catalyst. After cooling, the mixture was vacuum (~ 0.1 Torr) stripped at about 105°C for 4 h to remove

**Table II Characteristics of BTDA/*m*-BAPS-Based Poly(imide siloxane)s**

Sample Code	PIS 5Siy			PIS 7Siy			PIS 9Siy		
	Characteristics APPS/PIS Mol Ratio (%), “y”	Siloxane wt %	$\eta_{inh}^a$	Opacity <sup>b</sup>	Siloxane wt %	$\eta_{inh}^a$	Opacity <sup>b</sup>	Siloxane wt %	$\eta_{inh}^a$
0	0	0.77	—	0	0.77	—	0	0.77	—
0.6	0.8	0.68	—	1.1	0.65	—	1.6	0.65	+
1.1	1.5	0.67	—	2.0	0.62	+	2.9	0.61	+
1.7	2.2	0.64	—	3.2	0.60	+	4.3	0.60	+
2.7	3.6	0.65	+	5.0	0.64	+	6.9	0.60	++
4.2	5.2	0.60	+	7.7	0.56	++	10.4	0.56	++
6.1	— <sup>c</sup>	—	—	—	—	—	14.8	0.56	++
7.7	10.2	0.60	++	13.8	0.53	++	18.2	0.52	+++
10.0	—	—	—	17.6	0.49	+++	22.9	0.49	+++
13.7	—	—	—	23.5	0.50	+++	—	—	—
14.2	18.6	0.53	++	—	—	—	—	—	—
16.6	21.6	0.49	++	—	—	—	—	—	—
19.0	24.6	0.50	++	—	—	—	—	—	—

<sup>a</sup> The inherent viscosity was determined at a concentration of 0.5 g/dL of the polyamic acids in NMP at 25°C.

<sup>b</sup> The opacity was observed by bare eyes with the following classification: “—”; clear; “+”; slight cloudy; “++”: cloudy; “+++”: heavily cloudy.

<sup>c</sup> Not determined.

the residual D4. The number average molecular weight,  $M_n$ , determined by means of the proton nuclear magnetic resonance (NMR) spectroscopy,<sup>18</sup> is 507 g/mol. Similarly, the APPS oligomers of molecular weights 715 g/mol and 996 g/mol were synthesized by the same method with the appropriate mol ratio of DSX/D4 and with the same wt % of the catalyst in the reaction and their molecular weight also characterized with the proton NMR.

### Sample Preparation

Two types of poly(imide siloxane)s were synthesized, one from BTDA, *m*-BAPS and APPS ( $M_n$  = 507, 715, and 996 g/mol, respectively), and the other from PMDA, *p*-PDA, and APPS ( $M_n$  = 507 and 715 g/mol, respectively). The reaction is shown in Scheme II. The mol ratios of APPS to poly(imide siloxane), APPS/PIS, were 0, 0.1, 0.5, 0.6, 1.1, 1.7, 2.7, 4.2, 6.1, 7.7, 10.0, 13.7, 14.2, 16.6, and 19.0%, and the mol ratio of the total diamines to the dianhydride for the reactions was kept at 1 : 1. The mol of PIS are defined as the total mol number of the dianhydrides and the diamines.

The poly(imide siloxane)s made from APPS with the molecular weight of 507, 715, and 996 g/mol, respectively are designated as the codes PIS5Siy, PIS7Siy, and PIS9Siy, respectively,

and the “y” value stands for the mol ratio of APPS/PIS.

A three-neck 100-mL round-bottom flask was fitted with a mechanical stirrer, a nitrogen inlet, and a gas outlet. The flask was first purged by nitrogen gas and heated on a hot plate to remove the moisture. Then, the flask was cooled down to the ambient temperature under the nitrogen stream.

In a typical reaction to prepare PIS5Si0.6, 1.6110 g of BTDA (0.0050 mol) was added into the solution containing 2.1279 g of *m*-BAPS (0.00492 mol), 0.0414 g of APPS (0.00008 mol) and 10.7528 g of dry NMP. BTDA was introduced into the solution in five portions an hour apart. The poly(amic acid siloxane) (PAAS) solution was then stored in the freezer (about  $-15^\circ\text{C}$ ). Polymerizations were conducted at 15 and 26% solids content (w/w) for PMDA/*p*-PDA and BTDA/*m*-BAPS-based polyimides, respectively.

For the microscopic observation, the poly(amic acid siloxane) is spin coated on a clean glass slide and imidized in a vacuum oven at temperatures of 100, 150, 200, 250, and 300°C, each for 1 h.

For mechanical characteristic test, the poly(amic acid siloxane) solution was coated on a PET sheet with a thickness of 250  $\mu\text{m}$ . The PAAS was then heated at 100°C for 1 h in a forced-air con-

**Table III Characteristics of PMDA/*p*-PDA-Based Poly(imide siloxane)s**

Sample Code	PIS 5Siy			PIS 7Siy		
	wt %	$\eta_{inh}^a$	Opacity <sup>b</sup>	wt %	$\eta_{inh}^a$	Opacity <sup>b</sup>
Characteristics APPS/PIS Mol Ratio (%), "y"						
0	0	1.54	—	0	1.54	—
0.1	— <sup>c</sup>	—	—	0.6	0.61	++
0.5	1.4	0.68	++	—	—	—

<sup>a</sup> The inherent viscosity was determined at a concentration of 0.5 g/dL of the polyamic acids in NMP at 25°C.

<sup>b</sup> The opacity was observed by bare eyes with the following classification: "—": clear; "++": cloudy;

<sup>c</sup> Not determined.

vection oven to remove the solvent. The PAAS film was then transferred to a rectangle stainless frame clamp and imidized at temperatures of 150, 200, 250, and 300°C, each for 1 h. The thickness of PIS film was ranged from 28 to 32  $\mu\text{m}$ .

Similarly, other poly(imide siloxane)s with different mol ratios of APPS/PIS and molecular weights of APPS were also prepared by the same method.

### Measurements

The inherent viscosities ( $\eta_{inh}$ ) of the poly(amic acid siloxane)s were determined at a concentration of 0.5 g/dL in NMP thermostated at 25°C by an Ubbelohde viscometer with capillary sizes chosen to keep flow time greater than 120 s.

Dynamic mechanical properties of the poly(imide siloxane)s were determined using a TA Instruments DMA 2980 Dynamic Mechanical Analyzer at a heating rate of 2°C/min from -145 to 280°C. The samples (15 × 5 mm) were run at a frequency of 1 Hz with a film tension clamp. The stress-strain tests were also measured on the same

equipment with the TMA Controlled Force mode. The PIS samples (20 × 4 mm) were elongated at a ramp force of 4 Newtons per minute at room temperature and -118°C, respectively. The optical micrographs of the polyimide siloxane film were observed on an Olympus BHSM polarizing optical microscope.

The fractured surfaces of poly(imide siloxane) films, naturally broken during cooling in liquid nitrogen, were examined using a Hitachi S-4000 scanning electron microscope after prior vapor deposition of a thin gold film.

## RESULTS AND DISCUSSION

Poly(imide siloxane) is an important material in electronic packaging, especially in the Lead-on-Chip (LOC) Technology. It requires the material be heat stable, mechanically strong, and reasonably adhesive with the substrate in a short time (several seconds) on a hot press. Low pressing temperatures are desirable, and should not exceed 400°C. To reach effective adhesion in a short time the pressing temperature is normally 100–150°C higher than the  $T_g$  of the PIS.

Although siloxane incorporation in the polyimides can improve the interfacial adhesion with substrates, the incorporation of siloxane segment into the polyimide causes the drop of the  $T_g$  of the pristine polyimide (PI) and weakens the mechanical strength. For the LOC purpose, the PIS needs to contain as little siloxane as possible to maintain good adhesion. It is well known that the morphology of polymers affects their mechanical properties and adhesive characteristics. In this article, we first investigate the  $T_g$ s of the pristine PI and the solubility parameters of the pristine PI and pristine siloxane polyimide to choose a proper

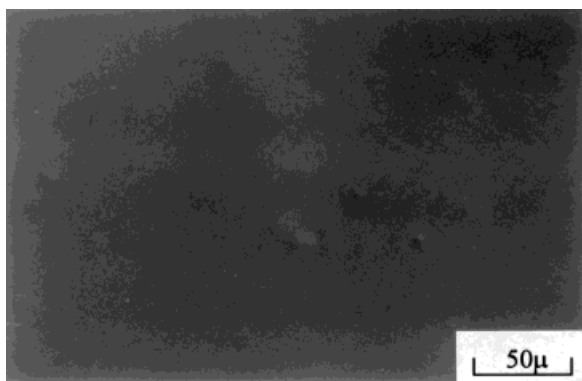


**Figure 1** POM micrographs of pristine BTDA/*m*-BAPS polyimide(unmodified).



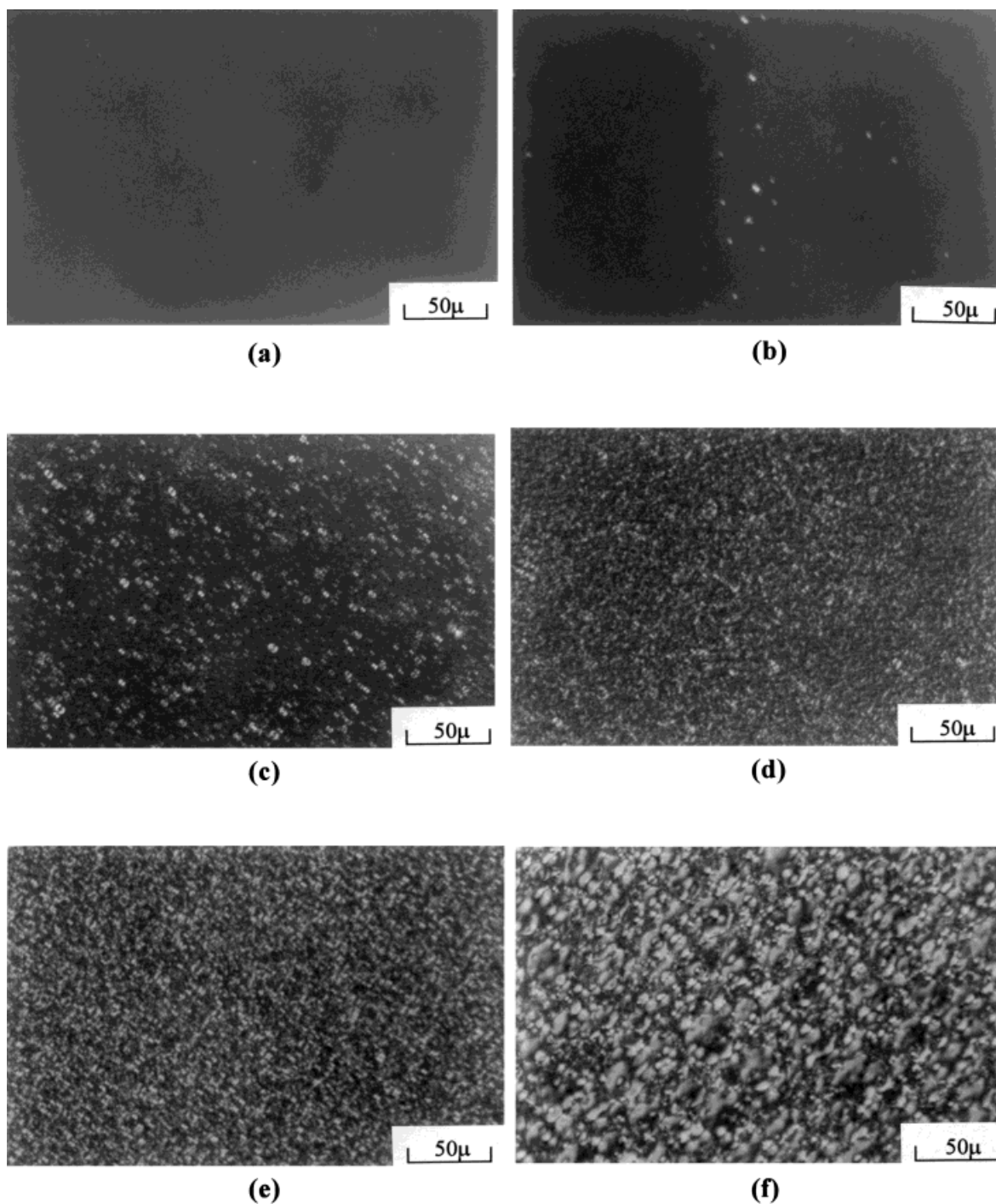


**Figure 2** POM micrographs of PIS5Si<sub>y</sub> films (BTDA/*m*-BAPS based) with the “y” value equal to: (a) 1.7%, (b) 2.7%, (c) 7.7%, (d) 14.2%, (e) 16.6%, (f) 19.0%.

system to make a systematic study on the siloxane effect on the morphology of the PIS.

Table I lists the estimated solubility parameters<sup>20</sup> and the  $T_g$ s of various pristine polyimides. It shows that the pristine siloxane polyimide has lower solubility parameter values than the other

pristine aromatic polyimides. Except for the fluorinated polyimides, the *m*-BAPS-based polyimides and *m*-BAPE-based polyimides have the lowest solubility parameters. The imides with low solubility parameter value are potentially miscible with the corresponding siloxane imide be-

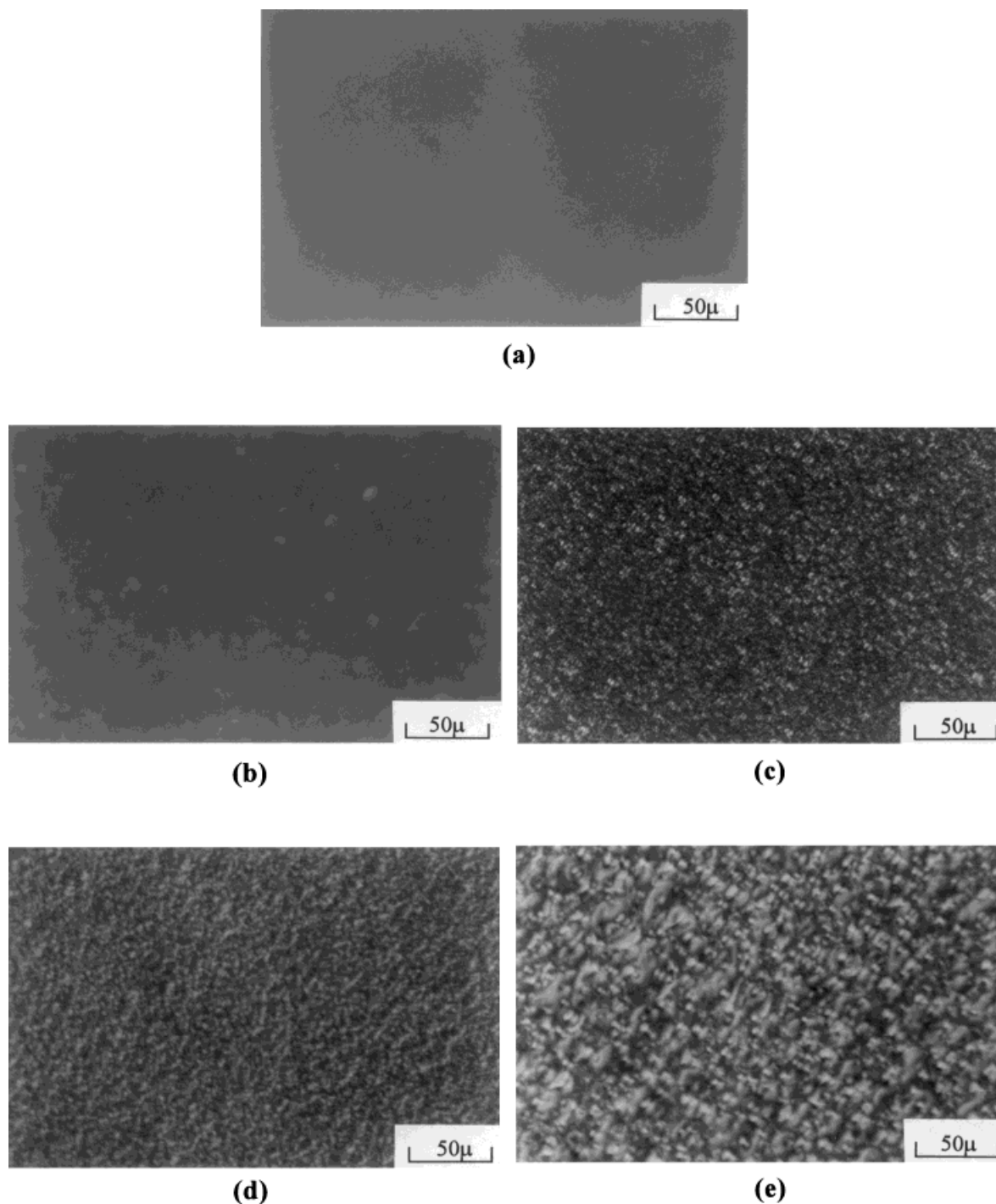


**Figure 3** POM micrographs of PIS7Si9 films (BTDA/*m*-BAPS based) with the “y” value equal to: (a) 0.6%, (b) 1.1%, (c) 7.7%, (d) 10.0%, (e) 13.7%.

cause of its low solubility parameter. However, the  $T_g$ s of the *m*-BAPS-based polyimides (from 254–211°C) are higher than those of the corresponding *m*-BAPE based polyimides (from 212–181°C). In considering the processing temperature, thermal property, the cost, and the avail-

ability, the BTDA/*m*-BAPS polyimides were chosen as the pristine polyimide to study the morphology of the poly(imide siloxane)s. PMDA/*p*-PDA pristine polyimide had the highest solubility parameter of all. Its poly(imide siloxane) morphology was also under investigation. The mor-

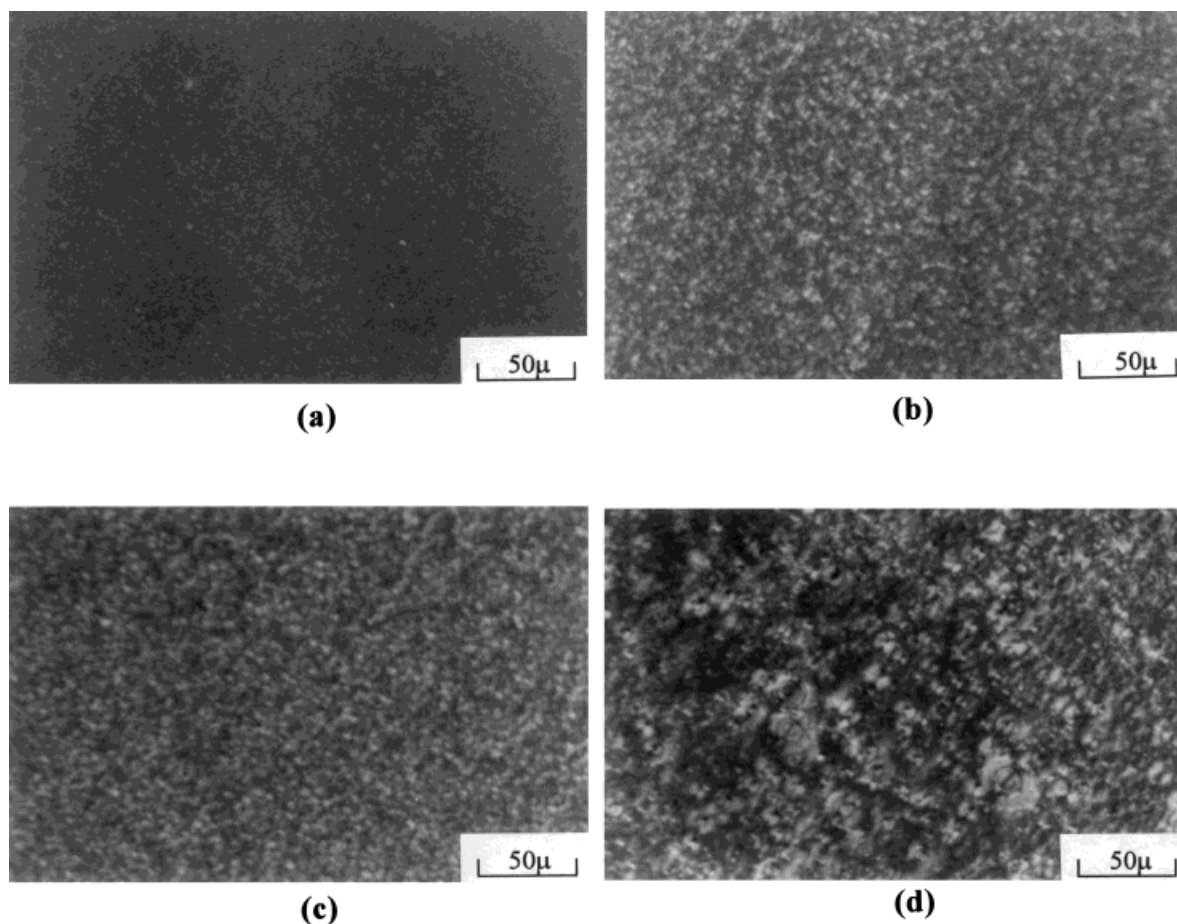


**Figure 4** POM micrographs of PIS9Siy films (BTDA/*m*-BAPS based) with the “y” value equal to: (a) 0.6%, (b) 6.1%, (c) 7.7%, (d) 10.0%.

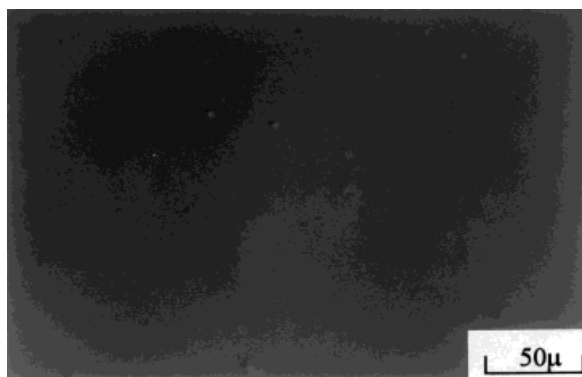
phology of the other types of poly(imide siloxane) may be deduced from the results.

The properties of BTDA/*m*-BAPS-based poly(imide siloxane) films are shown in Table II. The inherent viscosities of poly(amic acid siloxane)s ranged from 0.49 to 0.68 dL/g. The poly(imide siloxane)s had reasonably high molecular weight to form quality films. All the poly(imide siloxane)s cast formed a flexible films. As shown in Table II, the polymer films of PIS5Siy series are clear for APPS/PIS mole ratio “y” less than 2.7%. The PIS films become opaque when the “y” value  $\geq 2.7\%$ . On the other hand, the PIS films become opaque when the “y” value  $\geq 1.1\%$  in PIS7Siy films and “y” value  $\geq 0.6\%$  in PIS9Siy films. The weight percentages (wt %) of APPS in PISs at the critical condition of phase separation are 3.6, 2.0, and 1.6 wt % in PIS5Siy, PIS7Siy, and PIS9Siy, respectively. The critical condition of phase separation is observed at the lower mol ratio and at the lower weight percentage of APPS to PIS as the APPS

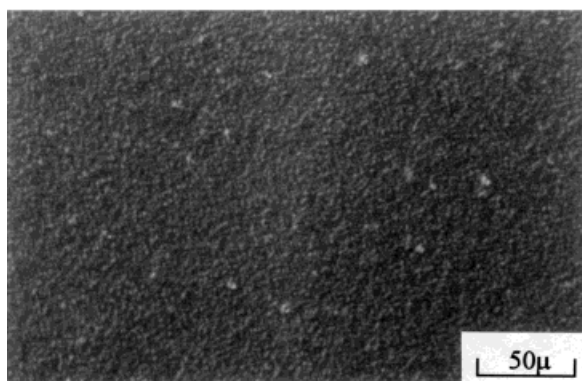
molecular weight increase. The higher molecular weight APPS easily leads to phase separation in the PIS film because the solubility parameter difference between the siloxane imide block and the BTDA/*m*-BAPS imide block increases with the APPS molecular weight. The data in Table III, exhibit that the PMDA/*p*-PDA-based PIS films are opaque, as the “y” value is equal to 0.5% and 0.1% for PIS5Siy and PIS7Siy, respectively. The critical condition is much lower than that in the corresponding BTDA/*m*-BAPS-based PIS films.

Micrographs of the unmodified BTDA/*m*-BAPS polyimide and its poly(imide siloxane) films taken by the polarizing optical microscope (POM) are shown in Figures 1–4. The POM micrograph of unmodified polyimide displays a homogeneous morphology (Fig. 1). In Figure 2, the morphology of the PIS5Siy films is homogeneous for “y” value less than 2.7%. As seen in Figures 2(b)–2(f), the APPS segments aggregate to form the dispersed phase as the APPS mol ratio  $\geq 2.7\%$ .

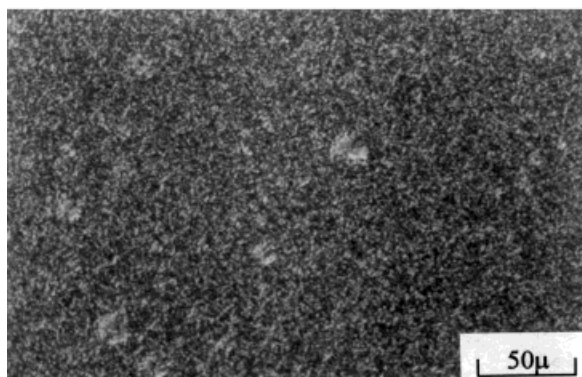




(a)



(b)



(c)

**Figure 5** POM micrographs of: (a) pristine PMDA/*p*-PDA unmodified polyimide, (b) PIS5Si0.5%, and (c) PIS7Si0.1% (PMDA/*p*-PDA based).

Similar results are found in Figures 3 and 4. The optical micrograph of PIS7Si0.6 film [Fig. 3(a)] does not show any phase separation. The domain formation in PIS7Si<sub>y</sub> and PIS9Si<sub>y</sub> polymer films are found at the “*y*” value  $\geq 1.1\%$  and

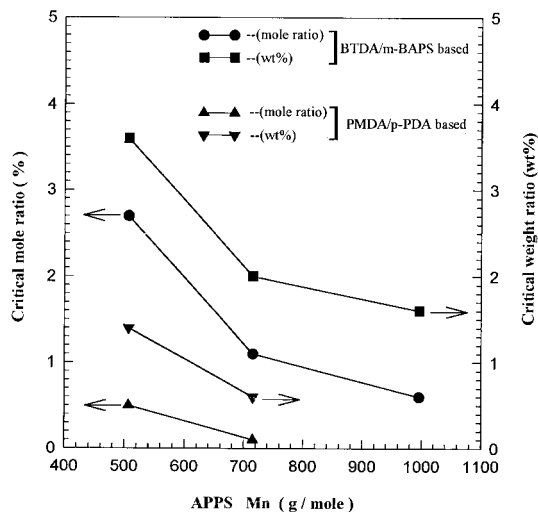


**Figure 6** The critical APPS/PIS mol ratio and wt % of phase separation as a function of molecular weight of APPS in poly(imide siloxane)s.

$\geq 0.6\%$ , respectively. The observed results are consistent with the result of the film opacity observation. The amount of the domains increases with APPS content in the PIS copolymers. Moreover, it is also found that the siloxane imide block in the poly(imide siloxane) film is the dispersed phase in all the PIS films until the mol ratio of APPS/PIS not less than 16.6, 10.0, and 7.7% in PIS5Si<sub>y</sub>, PIS7Si<sub>y</sub>, and PIS9Si<sub>y</sub>, respectively. As shown in Figures 2(e), 3(d), and 4(c), the siloxane imide blocks form a continuous phase in the PIS matrix. The siloxane imide blocks in the samples of PIS5Si14.2 [Fig. 2(d)], PIS7Si7.7 [Fig. 3(c)] and PIS9Si6.1 [Fig. 4(b)] partly interconnect with each other in addition to the existence of isolated domains.

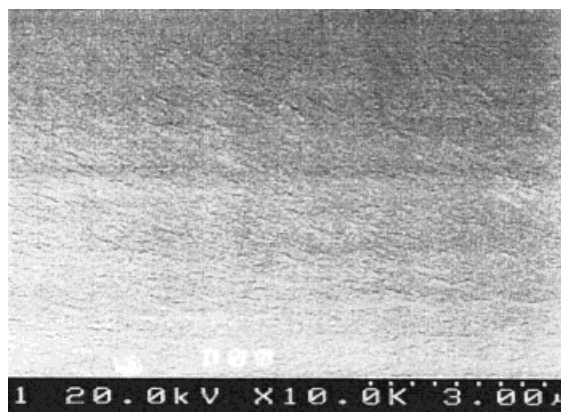


**Figure 7** SEM micrograph of fractured surface of pristine BTDA/*m*-BAPS polyimide (unmodified).

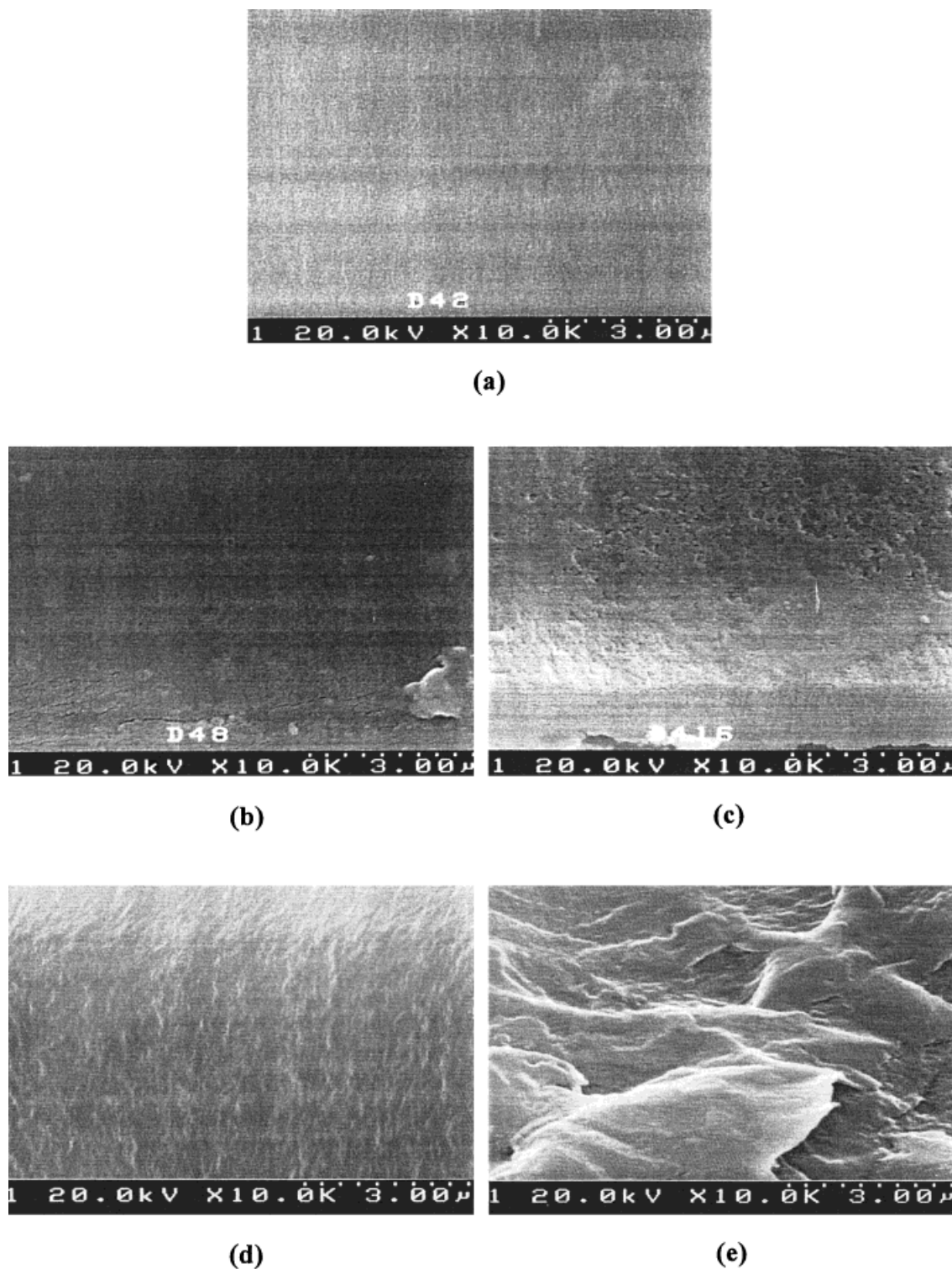


**Figure 8** SEM micrographs of fractured surfaces of PIS5Si<sub>y</sub> films (BTDA/*m*-BAPS based) with the “y” value equal to: (a) 1.7%, (b) 2.7%, (c) 7.7%, (d) 14.2%, (e) 16.6%.

POM micrographs of unmodified PMDA/*p*-PDA polyimide and its siloxane modified polyimides are shown in Figure 5. The POM micrograph of unmod-

ified PMDA/*p*-PDA polyimide displays a homogeneous morphology [Fig. 5(a)]. Figure 5(b) and (c) shows the micrographs of PIS5Si<sub>0.5</sub> and PIS7Si<sub>0.1</sub>

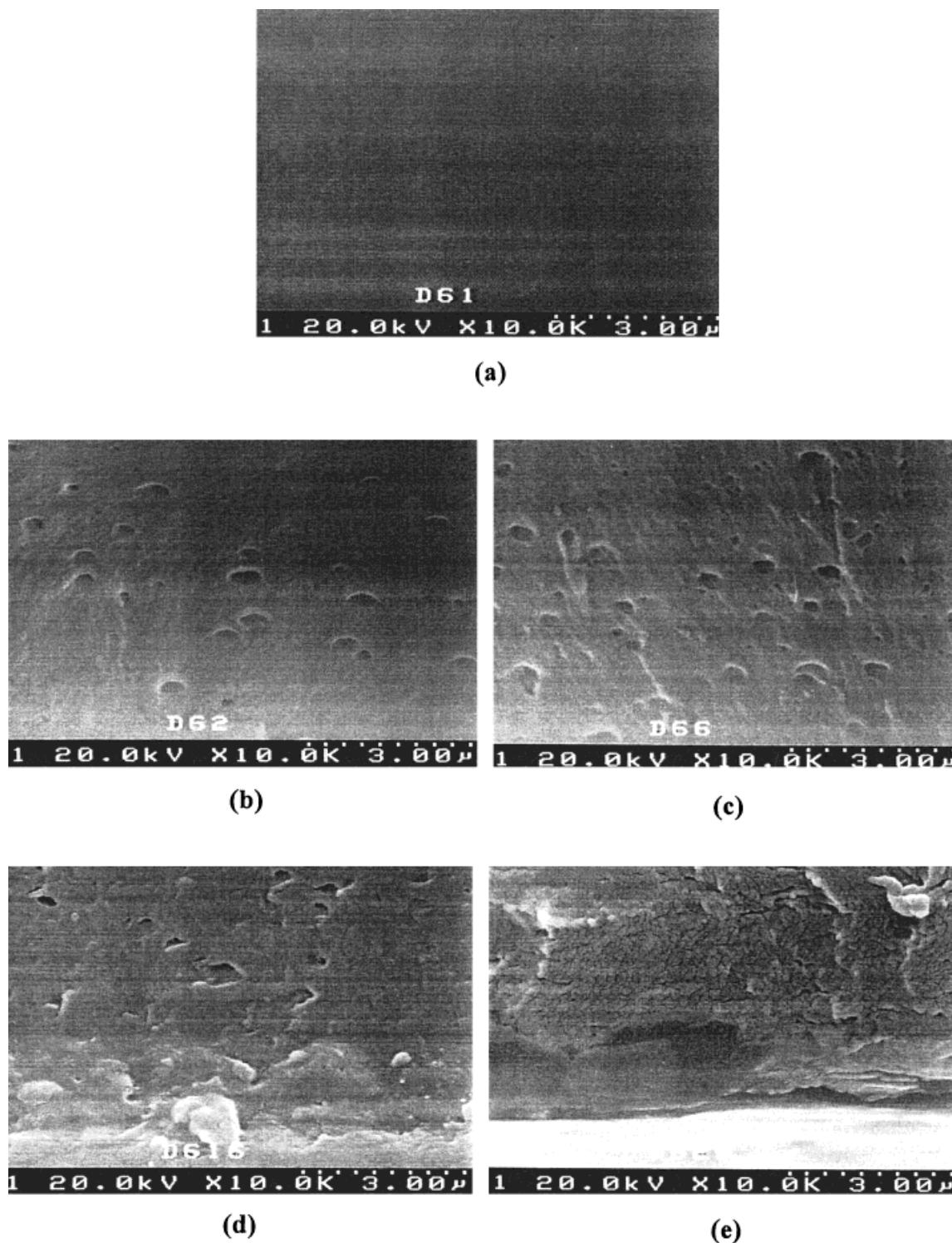
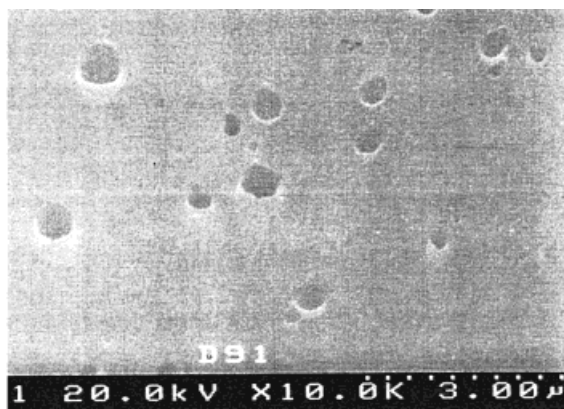


**Figure 9** SEM micrographs of fractured surfaces of PIS7Siy films (BTDA/*m*-BAPS based) with the “*y*” value equal to: (a) 0.6%, (b) 1.1%, (c) 2.7%, (d) 7.7%, (e) 10.0%.

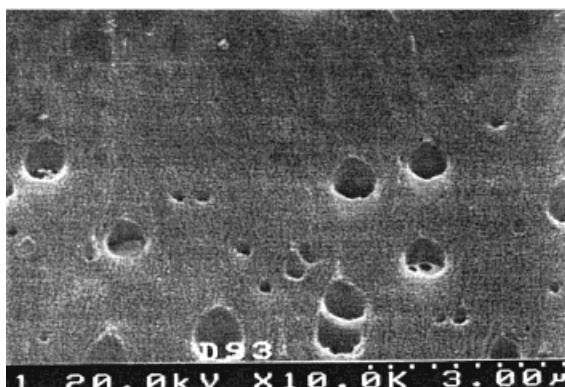
films, respectively. The siloxane imide blocks in both films aggregate and cause the phase separation at very low APPS content, 0.5 and 0.1 mol %, respectively. The critical “*y*” value for the phase

separation in PMDA/*p*-PDA-based poly(imide siloxane) films is much lower than that of the BTDA/*m*-BAPS-based PIS because the solubility parameter difference between the PMDA/*p*-PDA imide blocks

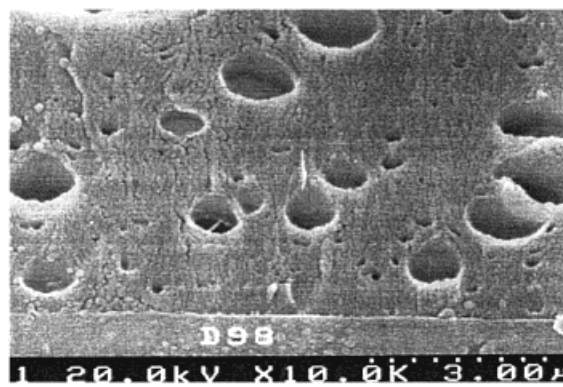




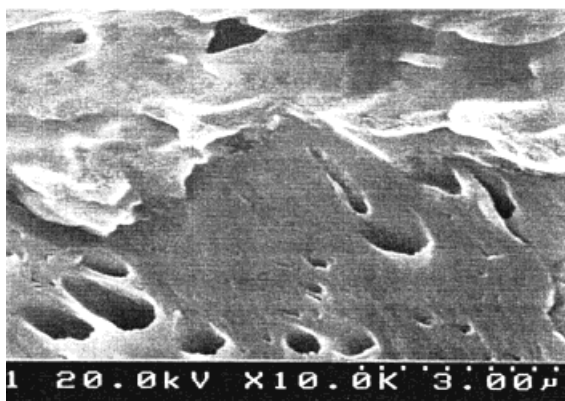
(a)



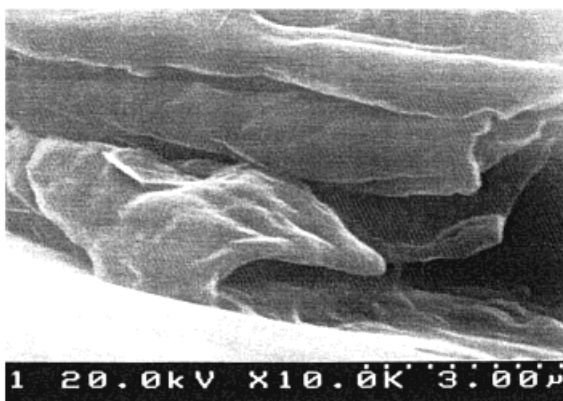
(b)



(c)



(d)



(e)

**Figure 10** SEM micrographs of fractured surfaces of PIS9Si $y$  films (BTDA/*m*-BAPS based) with the “*y*” value equal to: (a) 0.6%, (b) 1.7%, (c) 4.2%, (d) 6.1%, (e) 7.7%.

and the PMDA/siloxane imide blocks is greater than that between BTDA/*m*-BAPS imide blocks and the BTDA/siloxane imide blocks. The higher solu-

bility parameter of the pristine aromatic imide blocks causes the higher tendency of phase separation in the siloxane-modified polyimides.



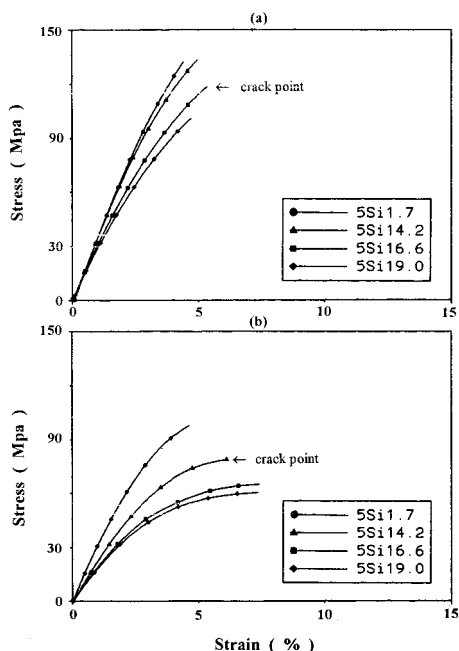


**Figure 11** Stress-strain curves of PIS5Si1.7, PIS5Si14.2, PIS5Si16.6, and PIS5Si19.0 films (BTDA/*m*-BAPS based) at different testing temperatures: (a)  $-118^{\circ}\text{C}$ , (b) room temperature.

The PMDA/*p*-PDA based PIS films also show the critical “*y*” value for the phase separation or the domain formation, depending on the segment

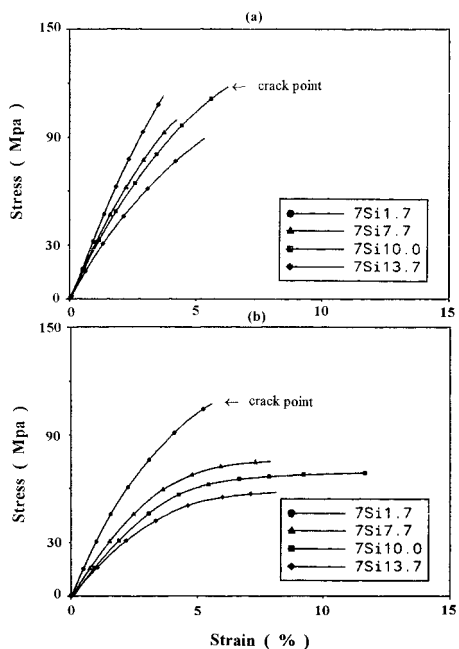


**Figure 12** Stress-strain curves of PIS7Si1.7, PIS7Si7.7, PIS7Si10.0, and PIS7Si13.7 films (BTDA/*m*-BAPS based) at different testing temperatures: (a)  $-118^{\circ}\text{C}$ , (b) room temperature.

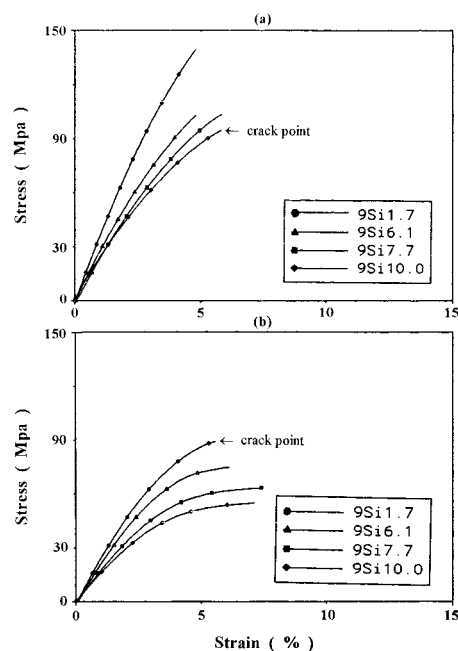


**Figure 13** Stress-strain curves of PIS9Si1.7, PIS9Si6.1, PIS9Si7.7, and PIS9Si10.0 films (BTDA/*m*-BAPS based) at different testing temperatures: (a)  $-118^{\circ}\text{C}$ , (b) room temperature.

length of the siloxane block in comparison between Figure 5(b) and (c). The effect of the molecular weight of APPS on the critical condition of the domain formation in the PMDA/*p*-PDA PIS films is more sensitive than in the BTDA/*m*-BAPS based PIS films.

Figure 6 shows the relationships between the APPS/PIS mol ratio and the molecular weight of APPS at the beginning of the domain formation observed from these PIS including BTDA/*m*-BAPS-based and PMDA/*p*-PDA-based copolymers. The result reveals that the critical domain formation of poly(imide siloxane) depends on both the molecular weight and the content of APPS at the same time. In other words, the aggregated domain can be formed even at a very low quantity of higher molecular weight APPS, and the domain is not observed for the lower molecular weight APPS at a higher content. It is also observed that the domain size tends to increase with the molecular weight of the APPS in the PIS, including BDTA/*m*-BAPS-based and PMDA/*p*-PDA-based PIS films, as shown in Figures 2–5.

The SEM micrographs of the fractured surface of the unmodified BTDA/*m*-BAPS polyimide, and the poly(imide siloxane) films with different mol ratios of APPS to PIS and different molecular weights of  $M_n = 507, 715, \text{ and } 996 \text{ g/mol}$  of

Table IV Ultimate Mechanical Properties of BTDA/*m*-BAPS-Based Poly(imide siloxane)s at Different Testing Temperatures from Dynamic Mechanical Analyzer

Sample Code	5Si <sub>y</sub>			7Si <sub>y</sub>			9Si <sub>y</sub>		
	At -118°C		At Room Temp.	At -118°C		At Room Temp.	At -118°C		At Room Temp.
Properties	Tensile Modulus (Gpa)	Strain at Break (%)	Tensile Modulus (Gpa)	Strain at Break (%)	Tensile Modulus (Gpa)	Strain at Break (%)	Tensile Modulus (Gpa)	Strain at Break (%)	Tensile Modulus (Gpa)
APPS/PIS Mol Ratio (%), "y"									
1.7	3.66	4.45	3.00	4.79	3.58	3.73	2.93	5.54	3.60
6.1	— <sup>a</sup>	—	—	—	—	—	—	—	2.70
7.7	—	—	—	—	2.91	4.33	2.03	7.89	2.49
10.0	—	—	—	—	2.77	6.26	1.74	11.74	2.44
13.7	—	—	—	—	2.30	5.30	1.51	8.16	—
14.2	3.37	4.88	2.23	6.26	—	—	—	—	—
16.6	2.98	5.36	1.84	7.17	—	—	—	—	—
19.0	2.82	4.70	1.76	7.16	—	—	—	—	—

<sup>a</sup> Not determined.

APPS are presented in Figures 7, 8, 9, and 10, respectively. The fractured surface of the pristine BTDA/*m*-BAPS polyimide (Fig. 7) is smooth. As shown in Figures 8–10, the fractured surfaces of the poly(imide siloxane) films PIS5Si<sub>y</sub> and PIS7Si<sub>y</sub> are also smooth at the low mol ratio of APPS to PIS, the "y" value. The fractured surfaces of PIS5Si1.7 [Fig. 8(a)] and PIS7Si0.6 [Fig. 9(a)] display a relatively smooth morphology, no domain observed. The fractured surfaces of PIS films become rough with holes or bumps on it as the "y" values  $\geq 2.7\%$ , 1.1%, and 0.6% for the PIS5Si<sub>y</sub>, PIS7Si<sub>y</sub>, and PIS9Si<sub>y</sub> series, respectively. The critical "y" values are the same as that observed in the POM micrographs. The holes or bumps are the siloxane-rich phases. It is noted from these SEM micrographs [Figs. 8(b)–(c), 9(b)–9(c), and 10(b)–(c)] that the dispersed domains are nearly spherical and the domain size increases with increasing the molecular weight of APPS at the same APPS/PIS mol ratio. Inspecting Figures 8(d), 9(d), and 10(d), it is interesting to see that the spherical siloxane-rich domains have been deformed, rather than spherical in shape, after fracturing in liquid nitrogen. Furthermore, the fractured surfaces of the samples PIS5Si16.6 [Fig. 8(e)], PIS7Si10.0 [Fig. 9(e)], and PIS9Si7.7 [Fig. 10(e)] exhibit a significant plastic deformation behavior. These reveal that the siloxane imide continuous phase, observing from POM, make the film ductile and deformable on fracturing. This phenomenon is attributed to increasing the flexibility of poly(imide siloxane) with the mol ratio of APPS to PIS and the APPS molecular weight.

The stress–strain curves of BTDA/*m*-BAPS-based poly(imide siloxane)s at room temperature and at -118°C (the  $T_{g1}$  in PIS9Si<sub>y</sub> samples) are shown in Figures 11–13, and the moduli and elongation of the PIS films are listed in Table IV. The data at -118°C and at room temperature display the similar trend: the elongation at break increases with the content of APPS and the modulus decreases with the increase of the APPS content. At low temperatures, the PIS films are relatively rigid with a higher modulus. In contrast, the PIS films exhibit tough behavior at room temperature, especially at the critical APPS content of the continuous siloxane-rich phase, such as PIS5Si16.6, PIS7Si10.0, and PIS9Si7.7. These PIS films exhibited the highest percent strain at break at RT. However, in each case the tough behavior does not increase as the APPS/PIS mol ratio ("y" value) exceeds the value of 16.6, 10.0, and 7.7%, respectively.

**Table V** The Transition Temperatures of BTDA/*m*-BAPS-Based Poly(imide siloxane)s from Dynamic Mechanical Analysis

Sample Code	5Siy			7Siy			9Siy		
	Characteristics APPS/PIS Mol Ratio (%), "y"	Siloxane wt %	$T_{g1}$	$T_{g2}$	Siloxane wt %	$T_{g1}$	$T_{g2}$	Siloxane wt %	$T_{g1}$
0	0	UD <sup>a</sup>	252	0	UD	252	0	UD	252
0.6	0.8	UD	251	1.1	UD	244	1.6	UD	244
1.1	1.5	UD	245	2.0	UD	244	2.9	-118	243
1.7	2.2	UD	241	3.2	-116	242	4.3	-118	241
2.7	3.6	UD	238	5.0	-116	240	6.9	-118	239
4.2	5.2	UD	232	7.7	-116	231	10.4	-118	237
6.1	— <sup>b</sup>	—	—	—	—	—	14.8	-118	236
7.7	10.2	-115	224	13.8	-116	231	18.2	-118	233
10.0	—	—	—	17.6	-116	229	22.9	-118	226
13.7	—	—	—	23.5	-116	220	—	—	—
14.2	18.6	-115	206	—	—	—	—	—	—
16.6	21.6	-115	195	—	—	—	—	—	—
19.0	24.6	-115	181	—	—	—	—	—	—

<sup>a</sup> UD means undetectable in the DMA.<sup>b</sup> Not determined.

The glass transition temperatures of the poly(imide siloxane)s from the dynamic mechanical analysis (DMA) are listed in Table V. It is found that the  $T_{g1}$  values, corresponding to the siloxane imide block or siloxane-rich phase, keep constant over different APPS contents. However, the  $T_{g2}$  values, corresponding to the  $T_g$  of the BTDA/*m*-BAPS imide-rich phase,<sup>13,15</sup> are a function of the APPS content. As expected, incorporating the APPS in the copolymer causes the decrease in the  $T_g$  of the BTDA/*m*-BAPS imide-rich phase. The detectable critical mol ratios of APPS to PIS for phase separation in the DMA measurement are 7.7, 1.7, and 1.1% for PIS5Siy, PIS7Siy, and PIS9Siy, respectively. In comparison to the polarizing optical microscope, and the scanning electron microscope, DMA is a less sensitive tool to detect the phase separation, the depression of the  $T_{g2}$  depends on the mol ratio "y" values. The results of DMA, although not shown in this article, also confirm that the storage modulus ( $G'$ ) of PIS films gradually decreases with increasing the APPS content. It means that the flexibility of PIS film increases with the content of APPS in the PIS.

## CONCLUSION

PMDA/*p*-PDA polyimide with a high-solubility parameter and BTDA/*m*-BAPS polyimide with a

high-solubility parameter and adequate  $T_g$  are chosen to understand the effect of the solubility parameter of the aromatic imide block in the poly(imide siloxane)s on the morphology of the PIS films. The effects of the APPS molecular weight and the APPS content on the phase separation, the morphology and the mechanical properties of the PIS films are systematically investigated. The systematic results will be helpful to understand the morphology of other poly(imide siloxane)s.

The domain formation of the poly(imide siloxane)s significantly depends on both the molecular weight and the content of APPS as well as the solubility parameters of the pristine aromatic polyimides (unmodified polyimides). The PMDA/*p*-PDA-based PIS films have much greater tendency toward the phase separation than the corresponding BTDA/*m*-BAPS-based PIS films. The phase separation (or domain formation) of PIS films in both POM and SEM micrographs are observed as the APPS content beyond the critical value. The isolated domains, siloxane-rich phase, may interconnect to form a continuous phase as the APPS content up to a certain value, which is also APPS molecular weight dependent. As the APPS with  $M_n = 507$  g/mol, the critical "y<sub>crit</sub>" values, the mol ratio of APPS/PIS, of the phase separation in PMDA/*p*-PDA-based PIS films and in BTDA/*m*-BAPS-based PIS films are 0.5 and 2.7%, respectively. As for the APPS with  $M_n = 715$  g/mol, the critical "y<sub>crit</sub>" values in both PIS

films are 0.1 and 1.1%, respectively. The PMDA/*p*-PDA-based PIS film is more sensitive to the phase separation. As the APPS molecular weight up to 996 g/mol, the critical “ $y_{crit}$ ” value in the BTDA/*m*-BAPS-based PIS film is down to 0.6%.

In the POM study, the continuous phases of the siloxane imide block can be observed in the PIS5Si16.6, PIS7Si10.0, and PIS9Si7.7 of BTDA/*m*-BAPS-based PIS films and the PIS film with the higher APPS content. In the SEM micrographs, the fractured surfaces of these PIS films with a continuous siloxane-rich phase show significant plastic deformation on naturally fracturing in the liquid nitrogen. At the lower APPS content, the fractured surfaces of the BTDA/*m*-BAPS-based PIS films have holes or bumps, and the size of the hole or bump increases with the APPS molecular weight. The data of the stress-strain test at  $-118^{\circ}\text{C}$  and at room temperature show that these BTDA/*m*-BAPS-based PIS films with a continuous siloxane-rich phase on its critical condition have the highest elongation of all in the same series of the PIS films. Further, increasing the siloxane APPS content does not improve the elongation of the PIS film. The PIS films having phase separation show two transitions  $T_{g1}$  at  $-118$ – $-115^{\circ}\text{C}$  and  $T_{g2}$  at  $181$ – $244^{\circ}\text{C}$  in the DMA. The first transition temperature kept constant does not change with the APPS content for the same series of the PIS films. This is due to the siloxane-rich phase. The second transition temperature depends on the APPS content. This is due to the aromatic imide phase. The DMA also confirms the tensile test result: the higher the APPS content, the lower the modulus of the PIS films.

The authors would like to express their appreciation to the National Science Council of the Republic of China and China Petroleum Company for financial support for this study under grant NSC 87-CPC-1-009-008.

## REFERENCES

1. Thompson, L. F.; Willson, C. G.; Tagawa, S., Eds. *Polymers for Microelectronics: Resists and Dielectrics*. American Chemical Society: Washington, DC, 1994.
2. Ghosh, M. K.; Mittal, K. L. Eds. *Polyimides: Fundamentals and Applications*. Marcel Dekker: New York, 1996.
3. Policastro, P. P.; Lupinski, J. H.; Hernandez, P. K. In *Polymeric Materials for Electronics Packaging and Interconnection*; Lupinski, J. H.; Moore, R. S., Eds.; American Chemical Society: Washington, DC, 1989, p. 140.
4. Okugawa, Y.; Yoshida, T.; Suzuki, T.; Nakayoshi, H. *IEEE* 1994, 570.
5. Sacher, E.; Klemberg-Sapieha, J. E.; Schreiber, H. P.; Wertheimer, M. R. *J Appl Polym Sci Appl Polym Symp* 1984, 38, 163.
6. Ying, L.; Edelman, R. 31st Natl SAMPE Symp 1986, 31, 1131.
7. St. Clair, A. K.; St. Clair, T. C. In *Polyimides: Synthesis, Characterization, and Applications*; Mittal, K. L., Ed.; Plenum Press: New York, 1984, p. 977, vol. 2.
8. Kaltenecker-Commercon, J. M.; Ward, T. C.; Gungor, A.; McGrath, J. E. *J Adhesion* 1994, 44, 85.
9. Cho, K.; Lee, D.; Ahn, T. O.; Seo, K. H.; Jeong, H. M. *J Adhesion Sci Technol* 1998, 12, 253.
10. Davis, G. C.; Heath, B. A.; Gildenblat, G. In *Polyimides: Synthesis, Characterization, and Applications*; Mittal, K. L., Ed.; Plenum Press: New York, 1984, p. 847, vol. 2.
11. Lee, Y. D.; Lu, C. C.; Lee, H. R. *J Appl Polym Sci* 1990, 41, 877.
12. Kuckertz, V. H. *Makromol Chem* 1966, 98, 101.
13. Summers, J. D., Ph.D. Dissertation, Virginia Polytechnic Institute and State University, Blacksburg, VA (1988).
14. Tsujita, Y.; Yoshimura, K.; Yoshimizu, H.; Takizawa, A.; Kinoshita, T. *Polymer* 1993, 34, 2597.
15. Riffle, J. S.; Yilgor, I.; Banthia, A. K.; Tran, C.; Wilkes, G. L.; McGrath, J. E. In *Epoxy Resin Chemistry II*; Bauer, R. S., Ed.; American Chemical Society: Washington, DC, 1983, p. 21, series 221.
16. Andolino Brandt, P. J.; Senger Elsbernd, C. L.; Patel, N.; York, G.; McGrath, J. E. *Polymer* 1990, 31, 180.
17. Gilbert, A. R.; Kantor, S. W. *J Polym Sci* 1959, 40, 35.
18. Summers, J. D.; Elsbernd, C. S.; Sormani, P. M.; Brandt, P. J. A.; Arnold, C. A.; Yilgor, I.; Riffle, J. S.; Kilic, S.; McGrath, J. E. In *Inorganic and Organometallic Polymer*; Zeldin, M.; Wynne, K. J.; Alcock, H. R., Eds.; American Chemical Society: Washington, DC, 1988, p. 360.
19. Wright, P. V. In *Ring-Opening Polymerization*; Ivin, K. J.; Saegusa, T., Eds.; Elsevier: New York, 1984, p. 1055, vol. 2.
20. Van Krevelen, D. W.; Hoftyzer, P. J. *Properties of Polymers*; Elsevier Scientific Publishing Co.: Amsterdam, 1976.
21. Tamai, S.; Yamaguchi, A.; Ohta, M. *Polymer* 1996, 37, 3683.
22. St. Clair, T. L.; St. Clair, A. K.; Smith, E. N. In *Structure-Solubility Relationships in Polymer*; Harries, F. W.; Seymour, R. B., Eds.; Academic Press: New York, 1977, p. 199.
23. Chung, T.-S.; Kafchinski, E. R. *Polymer* 1996, 37, 1635.